

Phase composition and properties of plasma-sprayed zirconia thermal barrier coatings

P. D. HARMSWORTH*, R. STEVENS

School of Materials, University of Leeds, Leeds LS2 9JT, UK

The use of X-ray diffraction combined with TEM analysis has been used to study the crystalline structure and change in phase composition of zirconia coatings containing 6–12 wt% Y_2O_3 . The optimum composition for maximum durability, observed for coatings within this composition range, is believed to be related to the microstructure developed on rapid cooling and to the volume fractions of t' , c and m phases formed during the evolution of the coating. The amount of these phases present in commercial thermal barrier coatings has been determined using X-ray diffraction and the mechanisms of toughening deduced from TEM examination of the sections of the coatings. The results obtained are discussed in relation to the degree of toughness and hence the thermal shock resistance which is a major factor in determining service life.

1. Phase composition of as-sprayed coatings

X-ray diffraction has been used to investigate the bulk phase composition of each of the coatings studied. This technique has been found to give the most accurate and reproducible analysis of phase composition [1] for zirconia, although considerable practical difficulties can arise and great care needs to be taken in both the experimental method and interpretation of results.

Low-angle X-ray diffraction analysis between 27° and 32° using standard peak intensity analysis [2] was used to assess the monoclinic phase content of the coatings, Table I. The amount of monoclinic phase can be seen to decrease from 10% in SCY6 to 5% in SCY8 (supplied by Magnesium Elektron Ltd, Manchester, UK) with no monoclinic detected in 10 or 12 wt% Y_2O_3 coatings. Examination of the relevant phase diagram [3, 4] suggests that the volume fraction of phases present is indicative of a non-equilibrium state. Indeed the yttria content of the zirconia alloys used for this study was such that compositions within the tetragonal plus cubic phase field would be ex-

pected. The situation becomes more complex in that a t' phase higher in Y_2O_3 content than the normal t phase exists and this t' phase appears to be relatively stable, i.e. it does not transform directly to monoclinic on cooling to room temperature.

High-angle analysis between 72° and 76° was subsequently used to resolve the cubic/ t' superimposed peaks, to give an indication of the cubic equilibrium tetragonal and metastable t' phase contents.

Only the $(400)t'$ and $(004)t'$ peaks were identified, the peak separation decreasing with increasing stabilizer addition as reported previously [4]. No evidence of the $(400)_c$ peak was observed. The linear decrease in tetragonal c/a ratio observed was used to calculate the change in Y_2O_3 content of the t' phase as done by Millar [3] and Scott [4], Table II. Fig. 1 shows the extension of these data in graphical form and gives a value for the Y_2O_3 content at which the coatings would be fully cubic at 16% $YO_{1.5}$ (14 wt% Y_2O_3). The single diffuse peak observed for 12 wt% yttria, therefore, is believed to arise from the superposition of two closely spaced t' peaks.

The K_{α_1} and K_{α_2} components of the t' peaks could not be resolved due to peak broadening arising from lack of compositional homogeneity in the ceramic coating, and the high internal stresses and small crystallite size [5]. The close proximity of lattice parameters combined with peak broadening makes quantitative analysis of t' and cubic phase contents very difficult requiring extensive peak resolution of XRD data. This process becomes increasingly difficult and less accurate at higher yttria contents. Even though a number of studies have attempted this work [6, 7], it is considered that any results obtained on the

TABLE I Low angle XRD analysis

	$(11\bar{1})_m$	2θ $(111)_m$	$(111)_{c/t'}$	$V_m\%$
SCY6	28.003	31.265	30.09	10.3
SCY8	28.05	31.35	30.06	5.05
10YSZ	–	–	30.04	–
12YSZ	–	–	30.02	–

* Present address: Tioxide Group plc, Central Laboratories, Portrack Lane, Stockton-on-Tees, UK.

TABLE II High angle XRD analysis

	c_t (nm)	a_t (nm)	a_c (nm)	$\Delta 2\theta_t$	c_t/a_t	wt % Y_2O_3 in t'
SCY6	0.5172	0.5112	—	1.013	1.0117	7.4
SCY8	0.5172	0.5124	—	0.788	1.0094	9.0
10YSZ	0.5164	0.5128	—	0.594	1.0070	11.0
12YSZ	—	—	(0.5136)	—	—	—

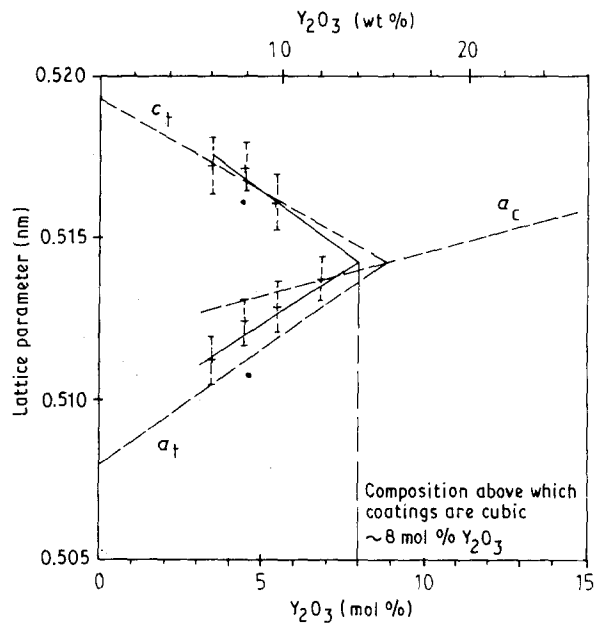


Figure 1 Variation of the t' lattice parameter with additive; showing composition at which coatings would be fully cubic, a comparison with lattice parameters from previous studies (---) [5], (●) [4], (—) present work.

present material would lead to uncertainties in their interpretation.

2. TEM analysis of phase composition

Recently, considerable work has been published on characterizing the high-ytria tetragonal or t' phase in ZrO_2 [8]. TEM analysis has been shown to be more effective in distinguishing between the cubic and t' phases in zirconia; it was therefore used for analysis of plasma-sprayed coatings. The larger grains $\sim 1 \mu m$ were found to be almost entirely t' - ZrO_2 , Fig. 2, the t' phase being differentiated from cubic by the presence of weaker forbidden reflections in the selected-area diffraction pattern [9, 10]. Clear evidence of t' tetragonal twins could be observed particularly in dark field when imaging one of the weak t' reflections. Also present within each of the twins are planar defects having the contrast and appearance of anti-phase domain boundaries (APBs) which are believed to be a characteristic feature of t' - ZrO_2 forming as a result of the c - t' transformation [11].

TEM analysis was also very useful in identifying the presence of monoclinic zirconia, the grains of which were highly twinned and faceted as a result of the martensitic transformation. Monoclinic ZrO_2 was clearly visible in both SCY6 and SCY8 compositions. However, it was also observed in both the 10 and

12 wt % Y_2O_3 samples. Fig. 3 shows a typical monoclinic grain. Transformation has initiated further transformation of adjacent grains, including partial transformation, an effect widely observed in TZP materials, an example of auto-catalytic transformation [12].

The 5%–6% volume expansion and shear strains associated with $t \rightarrow m$ transformation has resulted in the initiation of extensive microcracking in the sample. The complex layered microstructure of the thermal barrier coating then uses this feature to advantage when the microcracks propagate preferentially along the weaker grain-boundary phase described earlier. The convoluted path of the crack causes its termination within a short distance before it actually crosses the thickness of thermal barrier coating. During thermal cycling of the component the presence of such convoluted microcracks allows compliance of the strains developed in the ceramic by the differential thermal expansion of the coating and the substrate. The thermal cycling can thus take place without loss of the thermal barrier.

3. Microstructure–property relationships in as-received coatings

For improved coating performance in terms of maximum thermal cycle life the properties which need to be optimized can be summarized as: (1) good adhesion, (2) compliance with the substrate, (3) good thermal shock resistance. Microstructural features play a significant part in improving each of these properties and help explain reasons for the thermal cycle life observed in zirconia coatings.

3.1. Adhesion

The adhesive interfacial strength of the bond coat/ceramic interface has been found to be greater than the cohesive strength of the ceramic or the substrate/ceramic interface with no bond coat [8]. Cross-sectional TEM foils have demonstrated that an amorphous interfacial layer exists between the bond coat and the ceramic. This is believed to arise from the fusion and rapid solidification of the initially deposited ceramic material on the bond coat surface, possibly aided by the presence of SiO_2 and other impurities. The high strength of this amorphous interfacial film is believed to be responsible for the high adhesive strength. Fracture, when initiated at the interface, must follow a mix-mode path of lowest interfacial energy between the lamellae of the bond coat and the ceramic, which is normally observed [13]. Plastic deformation of

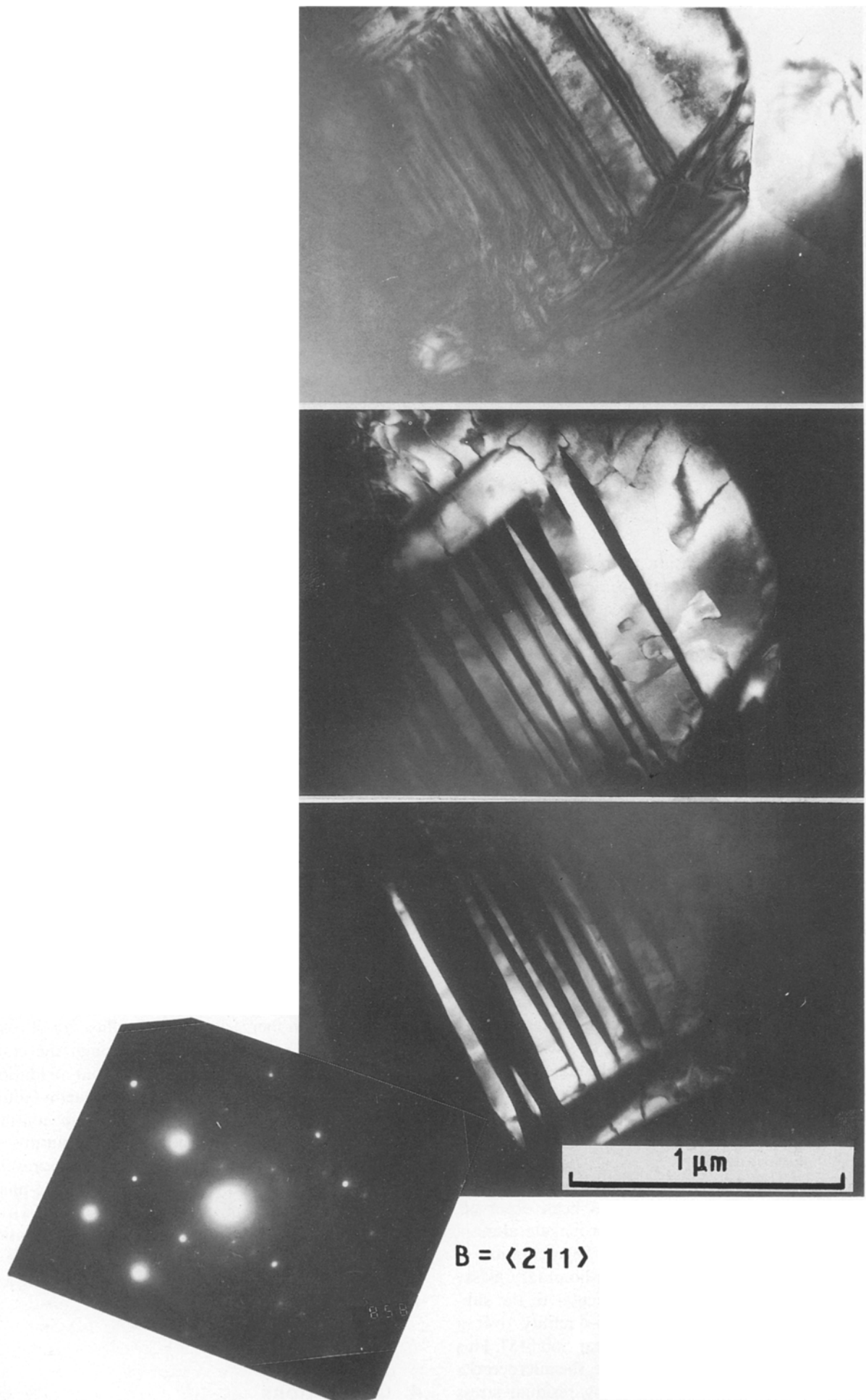


Figure 2 Transmission electron micrographs of the t' phase in ZrO_2 coatings showing t' tetragonal twins and the presence of APBs in (a) bright field, (b) dark field (1), (c) dark field (2).

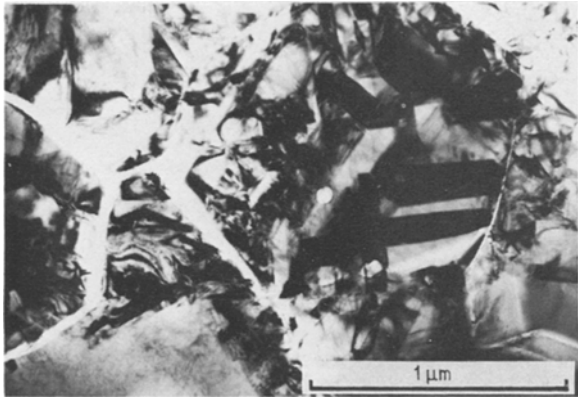


Figure 3 Transmission electron micrograph of the monoclinic phase in ZrO_2 coatings, showing crack branching and crack deflection resulting from transformation.

metallic lamellae in the MCrAlY bond layer then helps to increase the fracture toughness of the duplex arrangement.

3.2. Compliance

The high thermal expansion coefficient of the substrate material dictates that the ceramic coating must have the ability for a high degree of expansion, exceeding that of the bulk material. The discrepancy between the thermal expansion coefficient of the substrate and that of the bulk ceramic will result in high strains at the interface given by

$$\Delta e = (\alpha_1 - \alpha_2)\Delta T \quad (1)$$

where Δe is the strain developed, α_1 and α_2 are the thermal expansion of the substrate and ceramic, respectively, and ΔT is the change in temperature.

This strain can only be accommodated in the coating by developing a microstructure which possesses a high degree of compliance [14]. Compliance in the as-sprayed structure can be attained in two ways.

(i) The development of a lamellar structure aligned parallel to the substrate surface containing weak interlamellar bonding. These weak bonds are due to the presence of interlamellar porosity arising from plasma gas entrapment during spraying. Such features can reduce residual stress in the coating by shearing at the weak lamellar interface. However, the lamellae are not precisely oriented parallel to the substrate, being distorted by the shape of previously deposited material. This mechanism can therefore only act over a relatively short range.

(ii) Grain-boundary microcracking gives rise to interlamellar segmentation which has been observed. Microcracks have been shown to propagate along a weak grain-boundary glassy phase. Segmentation of the lamellae along the weaker grain-boundary glassy phase on a very fine scale perpendicular to the substrate gives the coatings a pseudo-ductility over a relatively large range of substrate expansion [15]. This allows free expansion of the substrate, the microcracks opening up during heating relieving residual stress and closing again during substrate contraction on cooldown [16].

3.3. Thermal shock resistance

The thermal shock resistance parameters of importance for ceramic coatings quenched from high temperature can be compared to those in refractory lining materials which already contain a high proportion of cracks. The thermal shock resistance, R''' , of these materials is described by Hasselman [17], where

$$R''' = \frac{E\gamma}{\sigma_f^2(1 - \mu)} \quad (2)$$

The most important parameter for improving the thermal shock resistance of the coatings is the toughness, γ , of the material. In ceramic materials having high toughness, cracks initiated during thermal shock may be arrested or prevented from causing catastrophic failure.

The mechanisms believed to be most effective in improving the thermal shock resistance in ceramic coatings are crack branching and crack deflection at transformed zirconia particles [18]. These toughening mechanisms have been observed, using TEM, in the ZrO_2 6 and 8 wt % coatings, and also in isolated instances in the 10 and 12 wt % Y_2O_3 coatings, Fig. 3.

The small degree of controlled $t \rightarrow m$ transformation, typically 5%–10%, is believed to be sufficient to relieve internal stresses in the coating and cause enough microcracking to improve the toughness. The prolonged thermal cycle life of coatings containing 6–10 wt % Y_2O_3 is therefore likely to be related to the improved toughness and thermal shock resistance. The optimum benefit to be obtained from such toughening mechanisms will be critically dependent on the amount of monoclinic phase in the as-received coating, which is governed mainly by the Y_2O_3 content. Compositions containing less than 6 wt % Y_2O_3 have been shown to contain insufficient stabilizer to form a fully t' structure [11]. This results in the formation of large amounts of the equilibrium low- Y_2O_3 t - ZrO_2 which readily transforms during thermal cycling to m - ZrO_2 . The volume expansion and shear displacement associated with this transformation gives rise to a rapid increase in the microcrack density and coating segmentation causing: (i) a degradation in the coating's thermal insulation resistance, and (ii) an increasing rate of diffusivity of oxidizing products to the bond coat through the crack paths, increasing the rate of bond coat oxidation, leading to rapid spallation and subsequent failure. Greater than 12 wt % yttria will result in coatings where the toughening mechanisms are all but absent. Cubic zirconia, or a very high- Y_2O_3 t' - ZrO_2 results, which rapidly forms a high proportion of single-phase c - ZrO_2 at elevated temperatures and contains virtually no m - ZrO_2 . The absence of any transformation toughening mechanism will subsequently give rise to poor thermal shock behaviour on thermal cycling and rapid spallation.

4. Conclusions

The volume fraction of individual phases in thermal barrier coatings of plasma-sprayed zirconia can be

determined by careful X-ray diffraction analysis, preferably used in conjunction with TEM.

The thermal shock resistance of the coatings can be improved particularly by increasing the coating toughness. In ZrO_2 thermal barrier coatings this is achieved by optimizing the toughening effect from crack branching and crack deflection as opposed to transformation toughening. Both phenomena are critically dependent upon the degree of $t \rightarrow m$ transformation. The coating composition having the optimum toughening capability was shown to correspond to ~ 8 wt % Y_2O_3 .

Acknowledgements

The support of SERC and Rolls Royce is appreciated, and particularly the help of Dr P. Morrell in providing specimens.

References

1. P. A. EVANS, R. STEVENS and J. G. P. BINNER, *Brit. Ceram. Trans. J.* **83** (1984) 39.
2. H. TORAYA, M. YOSHIMURA and S. SOMIYA, *J. Amer. Ceram. Soc.* **67** (1984) C-183.
3. R. A. MILLAR, R. G. SMIALEK and R. G. GARLICK, "Advances in Ceramics", Vol. 3, "Science and Technology of Zirconia" edited by A. H. Heuer and L. W. Stobbs (American Ceramic Society, Columbus, Ohio, 1981) p. 241.
4. H. G. SCOTT, *J. Mater. Sci.* **10** (1975) 1527.
5. B. D. CULLITY, "Elements of X-ray Diffraction" (Addison-Wesley, Reading, MA, 1956).
6. J. R. BRANDON and R. TAYLOR, in "Proceedings of the International Conference on Materials '87", London, 1987 (Institute of Metals, London) pp. 69-77.
7. N. RAVI SHANKAR, H. HERMAN and C. C. BERNDT, *Ceram. Engng Sci. Proc.* **4** (1983) 784.
8. R. CHAIM, M. RUHLE and A. H. HEUER, *J. Amer. Ceram. Soc.* **68** (1985) 427.
9. V. LANTERI, A. H. HEUER and T. E. MITCHEL, *Adv. Ceram.* **12** (1984) 118.
10. R. C. GARVIE, R. H. HANNINK and R. T. PASCOE, *Nature* **258** (1975) 703.
11. A. H. HEUER and M. RUHLE, "Advances in Ceramics", Vol. 12, "Science and Technology of Zirconia II" (American Ceramic Society, Columbus, Ohio) (1984) p. 1.
12. M. RUHLE, N. CLAUSSEN and A. H. HEUER, (eds), *ibid.* **12** (1984) 352.
13. G. W. HEINTZE and R. McPHERSON, "Advances in Ceramics", Vol. 24a, "Science and Technology of Zirconia III", (American Ceramic Society, Westerville, Ohio, 1986) p. 431.
14. C. C. BERNDT and H. HERMAN, "Proceedings of the 10th International Conference on Thermal Spraying, Essen, FRG, DVS (German Welding Society, 1983) pp. 175-179.
15. P. A. SIEMERS and R. L. MEHAN, *Ceram. Engng Sci. Proc.* **4** (1982) 828.
16. R. L. MULLEN, B. L. VLECK, R. C. HENDRICKS and G. M. McDONALD, *Ceram. Engng Sci. Proc.* **8** (1987) 582.
17. D. P. H. HASSELMAN, *J. Amer. Ceram. Soc.* **52** (1969) 600.
18. A. G. EVANS, *Adv. Ceram.* **12** (1984) 193.

Received 27 July
and accepted 9 August 1990